# VARIABILITY OF THE INHERENT AND APPARENT OPTICAL PROPERTIES IN A HIGHLY TURBID COASTAL AREA: IMPACT ON THE CALIBRATION OF REMOTE SENSING ALGORITHMS.

*Rosa Astoreca[1], Kevin Ruddick[2], Véronique Rousseau[1], Barbara Van Mol[2], Jean-Yves Parent[1] and Christiane Lancelot[1]*

1. Ecologie des Systèmes Aquatiques (ESA), Université Libre de Bruxelles, Campus Plaine - CP 221, Boulevard du Triomphe, B-1050 Brussels, Belgium; rastorec(at)ulb.ac.be
2. Management Unit of the North Sea Mathematical Models (MUMM), Royal Belgian Institute of Natural Sciences (RBINS), 100 Gulledelle, B-1200 Brussels, Belgium

## ABSTRACT

The Southern Bight of the North Sea is characterised by a large influence of river inputs, which results in significant eutrophication of the coastal area. High values of chlorophyll (CHL) and total suspended matter (TSM) have been reported for these waters, associated with blooms of different species and resuspension of bottom sediments. Optical properties vary considerably both seasonally and regionally. Considerable effort has been taken in the past years to retrieve CHL and TSM maps from satellite imagery. An optical characterisation of the area is essential for the understanding of the satellite imagery. In particular, algorithms for retrieval of CHL and TSM are based on assumptions regarding IOPs which may not be valid or may need to be modified for this region and/or for certain seasons.

For this purpose, extensive sampling of these water constituents was carried out in the Belgian and adjacent coastal areas, in different seasons during 2004. Inherent optical properties (IOPs): particulate, non-algal particle (NAP), phytoplankton and coloured dissolved organic matter (CDOM) absorption were measured spectrophotometrically, and an absorption meter for total absorption and particle scattering was used *in situ*. Simultaneously, the apparent optical property (AOP) water-leaving radiance reflectance has been measured with a system of TriOS spectroradiometers.

In this paper, we show some examples of the high variability of IOPs in the area and how it impacts the water-leaving reflectance, and hence retrieval of products such as CHL and TSM. The contribution of phytoplankton, CDOM and NAP has been shown to vary between coast and offshore and also between estuary and Atlantic-dominated waters. The impact of this variation is assessed for a red/NIR algorithm for CHL retrieval. The results show that neglecting CDOM and NAP absorption causes CHL overestimation at low CHL. Variation of CHL-specific phytoplankton absorption is also shown to be a key source of retrieval error. This is the first step to provide a regional calibration of the CHL retrieval algorithms for these highly turbid coastal waters and to precisely quantify the uncertainty of retrieval associated with variability in specific IOPs (SIOPs).

**Keywords:** Inherent optical properties, near infrared absorption, chlorophyll *a* retrieval, remote sensing algorithms.

## INTRODUCTION

The Southern Bight of the North Sea is a shallow sea region (depths up to 40 m) with strong semi-diurnal tidal currents and wind-driven currents. The coastal strip receives nutrient inputs from a number of rivers, which cause eutrophication of the area (1,2). This high nutrient input causes a shift in phytoplankton species composition, from diatom-dominated towards blooms of undesirable species such as the large colony-forming *Phaeocystis* in spring (3). The phytoplankton bloom is associated with high concentrations of chlorophyll *a* (CHL). High concentrations of total suspended matter (TSM) result primarily from resuspension of bottom sediments originating from the Channel (4) or from local erosion.

There is a need to monitor these blooms in order to assess the current eutrophication status of Southern Bight waters and monitor the results of future nutrient reduction policies. Due to the highly variable hydrodynamics of the area, remote sensing of ocean colour has been identified as a powerful tool for mapping the eutrophication status of the area.

For the validation and development of algorithms based on ocean colour remote sensing, a complete optical characterisation of the water masses is required. Understanding of the variability of inherent optical properties (IOPs), apparent optical properties (AOP, water-leaving reflectance) and water constituents is essential for correct retrieval of CHL and TSM. In the framework of several projects (5,6,7), the area has been extensively sampled for TSM, CHL and optical properties.

A family of algorithms using two or three red or near infrared (NIR) bands (8,9,10,11), typically using a ratio of reflectances at, for example, 664 nm and 708 nm has been proven to be effective in estimating CHL for high TSM, high CHL waters. For Belgian waters (12) and other coastal and inland waters (13), algorithms using two or three red or NIR bands have been found to give good retrieval for high CHL (e.g. >10 mg $m^{-3}$), but generally poor retrieval for low CHL.

The errors associated with CHL retrieval are assumed to arise from three possible sources. Reflectance measurement errors are more significant in low backscatter waters where red and NIR reflectance is low and measurement errors can become very significant (14). A second source of errors is related to the model relating reflectance to the IOPs, absorption and backscatter coefficients. Finally, errors arise from the assumptions regarding the IOPs. Red/NIR algorithms are derived assuming that only pure water and phytoplankton absorb at 664 nm, that only pure water absorbs at 708 and 778 nm and that phytoplankton absorption at 664 nm is proportional to CHL. Investigating this latter source of errors constitutes one of the aims of this work.

The objectives of this study are to characterise the variability of IOPs, demonstrate the impact of this variability on the reflectance spectra and determine how retrieval algorithms should be calibrated or modified to take account of this variability.

## METHODS

Sampling was conducted in Belgian and adjacent coastal waters during two campaigns in May and July 2004. The phytoplankton population was dominated mainly by large *Phaeocystis* colonies in May and by diatoms of various sizes in July. Sampling stations are reported in Figure 1.

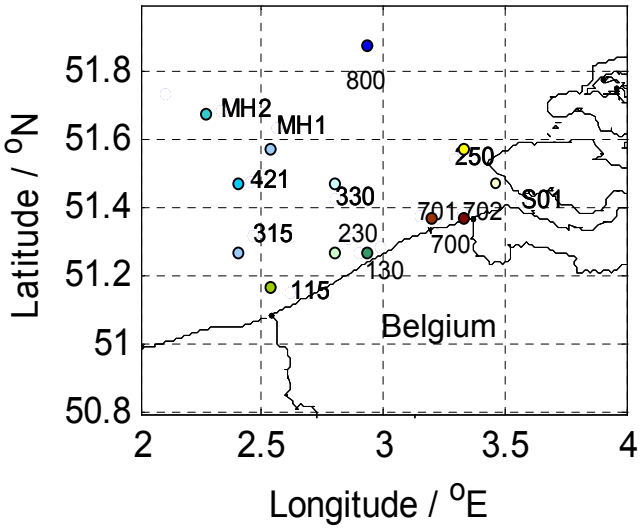


*Figure 1: Map of the Southern Bight of the North Sea showing the location of the sampling stations. The colour code shows blue for offshore stations and green-yellow-brown for coastal stations. The distinction for coastal stations is: brown, very turbid stations, yellow, stations in the estuary zone and green rest of coastal stations.*

At all stations, 20 L of sub-surface (0.5 m) seawater was sampled with a Niskin bottle. When *Phaeocystis* colonies were apparent, however, surface samples were taken with a bucket to avoid colony disruption. The following measurements were performed: particulate absorption, coloured dissolved organic matter (CDOM) absorption, chlorophyll *a* (CHL), total suspended particulate matter (TSM), phytoplankton community composition and ac-9 measurements. Filtrations (performed immediately after sampling) and ac-9 measurements were made from the 20 L sample. The protocols for each method are described in detail below.

**Particle, detrital (non-algal) and phytoplankton absorption**

Seawater was filtered onto a 25 mm glass fiber filter (Whatman GF/F), the volume varying with sample particle load from 0.05 to 1 L. Filters were kept in liquid nitrogen on board and then stored at -80°C in the laboratory until analysis. The absorbance spectra of particles $OD_P(\lambda)$ and non-algal particles $OD_{NAP}(\lambda)$ retained on the filter was determined following the Transmittance-Reflectance (T-R) method (15,16). Transmittance and reflectance were measured between 300 and 800 nm with a Uvikon 930 dual beam spectrophotometer equipped with a 6 cm-integrating sphere. Path length amplification was corrected using an algorithm which has been validated for several phytoplankton species and detrital particles (17). The filter was bleached with a solution of sodium hypochlorite (0.13% active chlorine) to obtain the absorbance spectrum of NAP including depigmented algal cells retained on the filter $OD_{NAP}(\lambda)$ (18). Absorbance values at each wavelength were converted into absorption coefficients as:

$$a_{P/NAP}(\lambda) = 2.303 \cdot OD_{P/NAP}(\lambda) / X \quad (1)$$

where $X$ is the ratio of filtered volume to the filter clearance area.

No correction to absorption for scattering in the NIR was performed since the T-R method has been proven to correct for scattering and because there is evidence that some mineral particles absorb in the NIR region (19).

The $a_{NAP}(\lambda)$ spectra were fitted to an exponential function for data between 340 and 750 nm:

$$a_{NAP}(\lambda) = a_{NAP}(\lambda_r) \cdot e^{\left(-S_{NAP}(\lambda - \lambda_r)\right)} \quad (2)$$

where $a_{NAP}(\lambda_r)$ is the absorption estimate at a reference wavelength (442 nm in this case) and $S_{NAP}$ is the slope of the curve.

The phytoplankton absorption coefficient $a_{ph}(\lambda)$ was obtained from

$$a_{ph}(\lambda) = a_P(\lambda) - a_{NAP}(\lambda) \quad (3)$$

**Specific inherent optical properties (SIOPs)**

The TSM-specific absorption coefficient $a^*_{NAP}(\lambda)$ was obtained from

$$a^*_{NAP}(\lambda) = a_{NAP}(\lambda) / TSM \quad (4)$$

The CHL-specific phytoplankton absorption coefficient $a^*_{ph}(\lambda)$ was obtained from

$$a^*_{ph}(\lambda) = a_{ph}(\lambda) / CHL \quad (5)$$

**CDOM absorption**

Some 100 ml of seawater were filtered through a 0.2 µm Nuclepore polycarbonate membrane, which was prefiltered with 100 ml of Milli-Q water. This filtrate was used to pre-wash a clean amber bottle and was then discarded. A second volume was filtered and kept at 4°C. Care was taken to use only clean glass combusted material to avoid any organic contamination of the sample.

The absorbance of the filtered water was measured in a Uvikon 930 dual beam spectrophotometer between 300 and 800 nm, using a 10 cm quartz cuvette (20). An air versus air baseline was recorded and was checked to be within ±0.0005 absorbance units. The absorbance spectrum of

Milli-Q water was used as reference and was subtracted from the sample absorbance to obtain the absorbance of the CDOM, $OD_{CDOM}(\lambda)$. No correction was applied to the data. The absorbance values at each wavelength were transformed into absorption coefficients using:

$$a_{CDOM}(\lambda) = 2.303 \cdot OD_{CDOM}(\lambda)/L \quad (6)$$

where $L$ is the length of the cuvette.

An exponential function was fitted to the data by nonlinear regression between 350 and 500 nm:

$$a_{CDOM}(\lambda) = a_{CDOM}(\lambda_r) \cdot e^{\left(-S_{CDOM}(\lambda-\lambda_r)\right)} \quad (7)$$

where $a_{CDOM}(\lambda_r)$ is the CDOM absorption estimate at a reference wavelength (442 nm in this case) and $S_{CDOM}$ is the slope of the curve.

**ac-9 measurements**

At all stations total non-water absorption $a(\lambda)$ and beam attenuation $c(\lambda)$ coefficients were measured with an ac-9 profiler (WetLabs, Inc). The instrument measures at the following 9 bands: 412, 440, 488, 510, 555, 630, 650, 676 and 715 nm.

The ac-9 was placed vertically in a thermoregulated bath with circulating seawater, in the wet lab of the ship. Water was pumped from a 20 L bottle sample previously rinsed and filled with surface seawater. Data were recorded during 2 minutes, and then the median was taken over 0.5-minute noise-free data. Temperature and salinity corrections were performed on the raw data (21). Absorption was corrected also for scattering by subtracting $a(715)$ from $a(\lambda)$ (22).

The particle scattering coefficient $b_p(\lambda)$ is obtained from

$$b_p(\lambda) = c(\lambda) - a(\lambda) \quad (8)$$

A pure water calibration was performed daily using freshly produced Milli-Q water to check for deviations from the annual WetLabs calibration (23).

**CHL and TSM.**

Between 0.05 and 1 L of seawater were filtered onto 25 mm glass fiber filters (Whatman GF/F) for HPLC CHL determination. The filters were kept in liquid nitrogen on board and then stored at -80°C in the laboratory until analysis. HPLC CHL concentration (mg/m$^3$) was detected by absorption at 436 nm and identified based on comparison of the retention time and spectra with standards (20).

Seawater (0.5 - 1 L) was filtered onto pre-weighed 47 mm 0.6 µm Nuclepore membranes for TSM determination. The filters were kept frozen at -20°C until analysis. The filters were dried at 105°C for 10 h and TSM concentration (g/m$^3$) was determined by gravimetry (20).

**Reflectance**

Water-leaving radiance reflectance is calculated from simultaneous above-water measurements of downwelling irradiance, $E_d^{0+}$, upwelling radiance at a zenith angle of 40°, $L_{sea}^{0+}$, and sky radiance, $L_{sky}^{0+}$, in the direction of the region of sky which reflects into the sea-viewing sensor, by:

$$\rho_w^{0+} = \pi \frac{L_{sea}^{0+} - \rho_{sky} L_{sky}^{0+}}{E_d^{0+}} \quad (9)$$

where $\rho_{sky}$ is the air-water interface reflection coefficient for radiance. This corresponds to *Method 1* of the NASA protocols (24). The measurements are made with a system of three TriOS-RAMSES hyperspectral spectroradiometers, two measuring radiance and one measuring downwelling irradiance. The instruments are mounted on a steel frame; zenith and nadir angles, respectively of the sea- and sky-viewing radiance sensors are 40°. The frame is fixed to the prow of the ship, facing forward to minimise ship shadow and reflection. The ship is manoeuvred on station to

point the radiance sensors at a relative azimuth angle of 135° away from the sun. More information on this system and on data processing is available in (25). $\rho_{sky}$ is estimated as a function of wind speed ($W$) by:

$$\rho_{sky} = 0.0256 + 0.00039\,W + 0.000034\,W^2 \quad \text{for} \quad \frac{L_{sky}^{0+}(750)}{E_d^{0+}(750)} < 0.05 \quad \text{(sunny)} \qquad (10)$$

$$\rho_{sky} = 0.0256 \quad \text{for} \quad \frac{L_{sky}^{0+}(750)}{E_d^{0+}(750)} \geq 0.05 \quad \text{(clouded)} \qquad (10a)$$

**Red/NIR ratio CHL algorithms**

The algorithm considered in this study is that defined for MERIS wavebands (10,26):

$$a_{ph}(664) = \frac{\rho_w(708)}{\rho_w(664)}\left(a_w(708) + b_b\right) - a_w(664) - \left(b_b\right)^p \qquad (11)$$

Where $\rho_w(664)$ and $\rho_w(708)$ are the (above-water) water-leaving radiance reflectances at 664 and 708 nm, $a_w(664)$ and $a_w(708)$ are the pure water absorption coefficients at 664 and 708 nm, $a_{ph}(664)$ is the phytoplankton absorption coefficient at 664 nm, and $p$ is an empirical constant. Parameter $b_b$ is an estimate of the backscatter coefficient obtained from:

$$b_b = \frac{a_w(778)\,\alpha\,\rho_w(778)}{\gamma' - \alpha\,\rho_w(778)} \qquad (12)$$

where $\rho_w(708)$ and $a_w(778)$ are the water-leaving reflectance and pure water absorption coefficient at 778 nm, $\alpha$=0.60 is a factor relating to refraction and reflection at the water surface and $\gamma'$=0.082 is an empirical constant of the reflectance-IOP model that has been used to derive this algorithm and is similar to the $I_1$ constant of (27). CHL concentration is then obtained simply from Eq. (11) by assuming a linear relationship between $a_{ph}(664)$ and CHL:

$$CHL = \frac{a_{ph}(664)}{a_{ph}^*(664)} \qquad (13)$$

where $a_{ph}^*(664)$ is the chlorophyll-specific phytoplankton absorption coefficient at 664 nm. In fact, this is an algorithm for retrieval of the optical parameter $a_{ph}(664)$, which is then converted to *CHL*.

Calibration of this algorithm using shipborne reflectance and *CHL* data obtained for the Ijssel lagoon (9) yielded the values: $a_{ph}^*(664) = 0.016\ \text{m}^2\ \text{mg}^{-1}$ and $p$=1.06. Laboratory data give $a_w(664)$=0.40 m$^{-1}$, $a_w(708)$=0.70 m$^{-1}$, $a_w(778)$=2.69 m$^{-1}$ (28). Thus, using Eqs. (11) - (13), *CHL* can be estimated from input reflectance data $\rho_w(664)$, $\rho_w(708)$ and $\rho_w(778)$.

**Simulations for impact of CDOM and NAP absorption**

To remove the non-IOP-related retrieval errors, simulations have been performed with reflectance data generated from the reflectance-IOP model used as basis for the algorithm described above. Thus, it is assumed that:

$$\alpha\rho_w(\lambda) = \gamma' \frac{b_b}{a_{tot}(\lambda) + b_b} \qquad (14)$$

where $\rho_w(\lambda)$ and the total absorption coefficient, $a_{tot}(\lambda)$, vary with wavelength, $\lambda$, but total backscatter coefficient, $b_b$, is assumed wavelength-independent over the spectral range considered. Parameters $\alpha$ and $\gamma'$ are used as for retrieval. $a_{tot}$ can be decomposed into constituents:

$$a_{tot}(\lambda) = a_w(\lambda) + a_{ph}(\lambda) + a_{CDOM}(\lambda) + a_{NAP}(\lambda) \qquad (15)$$

where $a_w(\lambda)$ data are identical to those used for retrieval.

Simulations are then performed as follows:

Input data consist of measured data $a_{ph}^{m}(\lambda)$, $a_{CDOM}^{m}(\lambda)$ and $a_{NAP}^{m}(\lambda)$ obtained as described in the preceding section. Measured $\rho_w(778)$ is also used as input (provided it is positive). From $\rho_w(778)$ the simulation input $b_b^{in}$ is calculated using Eq. (12). Thus, the IOPs $a_{tot}^{m}(\lambda)$ and $b_b^{in}$ form the complete input for these simulations.

From the IOP data, reflectance data are simulated for 664 nm, 708 nm and 778 nm using Eq. (14).

Then, a "retrieved" $a_{ph}^{ret}(664)$ is calculated from Eqs. (12) and (11). To avoid inconsistency between the forward and inverse models used here, $p$ is set equal to 1.0 for this step.

Now, if $a_{CDOM}^{m}(\lambda)$ and $a_{NAP}^{m}(\lambda)$ for 664 nm, 708 nm and 778 nm are set to zero and $a_{ph}^{m}(\lambda)$ is set to zero for 708 nm and 778 nm as assumed in the algorithm development, then the retrieval of phytoplankton absorption will be perfectly equal to the simulation input $a_{ph}^{ret}(\lambda)=a_{ph}^{m}(\lambda)$. Any difference between input and retrieved values then results entirely from non-zero $a_{CDOM}^{m}(\lambda)$ and $a_{NAP}^{m}(\lambda)$.

**Statistical analyses**

A one-way ANOVA test was conducted on the logarithmic-transformed data (IOPs, SIOPs) for comparison between seasons (May and July) and coast-offshore variability. The coast-offshore separation was based on distance from the shore with coastal stations defined as those within few km off the coast (Figure 1). The significant results were taken at $p<0.05$.

## RESULTS

### Variability in water constituents

The variation in the main water constituents is shown in Table 1 along with temperature and salinity of the water. CHL concentration is 5 fold higher in May at the end of the *Phaeocystis* spring bloom than in summer when maxima reach only 11.1 mg/m$^3$. The range of TSM and CDOM concentrations show no variation between spring and summer. Maximum values of CHL and TSM correspond to stations 130 in spring and 701 in summer (Figure 1). Maximum values of CDOM correspond to stations 700 in spring and S01 in summer (Figure 1).

*Table 1: Characteristics of the water masses during the May and July cruises. Mean value in brackets.*

| Cruise | Season | T /°C | S | CHL / mg/m$^3$ | TSM / g/m$^3$ | $a_{CDOM}(442)$ / 1/m |
|---|---|---|---|---|---|---|
| May 2004 | Spring | 10.34 - 12.60 | 31.15- 34.84 | 1.7 - 71.5 (16.2) | 1.8 - 34.0 (11.7) | 0.15- 0.45 (0.26) |
| July 2004 | summer | 15.44 - 17.51 | 31.43- 34.81 | 0.6 - 11.1 (4.0) | 3.1 - 37.4 (12.4) | 0.17- 0.50 (0.32) |

### Variability in the Inherent Optical Properties (IOPs)

A summary of the average IOPs for both cruises is given in Table 2. The $a_{ph}$ and $a_{NAP}$ data show higher values in spring than in summer. The maximum values are found at the coast: stations 130 and 700 in spring and stations 700, 701 and S01 in summer. The shape of the spectra changes between cruises reflecting the different pigment composition in the water (Figure 2). In May, $a_{ph}$ spectra show well defined peaks at 440, 461 and 676 nm corresponding to the *Phaeocystis* bloom as deduced from comparison with spectra of cultured *Phaeocystis* (not shown). In July, the peaks are defined around 440 and 676 nm, indicating a diatom-dominated phytoplankton community. Similar results were obtained in the Labrador Sea with prymnesiophytes having higher absorption coefficients than diatoms in the blue part of the spectrum (29). The main differences in the shape of the spectra for both cruises are found between 500 and 575 nm, a region where carotenoids, especially fucoxanthin, have their maximum absorption (30). The slope of the $a_{NAP}$ spectra for both cruises (Table 2) is close to that found for the North Sea (6) (0.0116/nm), but slopes of the $a_{CDOM}$

spectra are lower than the average (0.0167/nm) found in that study. $S_{NAP}$ shows no variation between cruises; neither does $S_{CDOM}$, which has the higher values (Figure 3). Variability in $S_{CDOM}$ is associated with changes in the composition of the CDOM pool, of which one source is associated with autochthonous production and the other one has a terrestrial origin (31). In this study the variability of $S_{CDOM}$ is low, suggesting that the composition of CDOM between seasons does not change significantly.

From Figure 3 it is clear that there is significant absorption of light by particles in the NIR region of the spectrum. This can be as high as 0.317 /m for $a_{NAP}(778)$ in May. However, the methodology used to measure these absorption coefficients is also known to have quite a large uncertainty at low absorption values due to the scattering error. Not all light scattered from the sample is detected by the instrument, leading to overestimation of the measured absorption. Some contrasting results have been found by different authors. In one study (32), it was concluded that the absorption by various types of marine particles in the NIR is generally negligible, while another study (19) concludes that marine samples show varying absorption in the NIR, depending on the importance and type of detrital fraction.

Regarding the high CDOM absorption in the NIR, there could be a methodological error involved in this measurement which arises from temperature and salinity differences between the sample and the Milli-Q water used as reference (21), during the measurement. These differences are more pronounced in the red part of the spectrum, especially around 750 nm, where for a 1°C temperature change there is a 0.36% change in the absorption coefficient of water (21). The consequences of this error on CHL retrieval are discussed below.

*Table 2: Average IOPs: phytoplankton, NAP and CDOM absorption coefficient at 442 nm and average slopes of the NAP and CDOM spectra for different locations during the May and July cruises. Standard deviations show the variability.*

| Cruise | Location | $a_{ph}(442)$ / 1/m | $a_{NAP}(442)$ / 1/m | $S_{NAP}$ / 1/nm | $a_{CDOM}(442)$ / 1/m | $S_{CDOM}$ / 1/nm |
|---|---|---|---|---|---|---|
| May 2004 | Coast | 0.48± 0.63 | 0.64± 0.43 | 0.0095± 0.0005 | 0.32± 0.14 | 0.0127± 0.0032 |
| | Offshore | 0.08± 0.04 | 0.12± 0.04 | 0.0100± 0.0011 | 0.20± 0.04 | 0.0108± 0.0024 |
| | all | 0.24± 0.39 | 0.32± 0.35 | 0.0100± 0.0008 | 0.23± 0.11 | 0.0121± 0.0028 |
| July 2004 | Coast | 0.21± 0.14 | 0.33± 0.24 | 0.0124± 0.0010 | 0.37± 0.08 | 0.0145± 0.0007 |
| | offshore | 0.05± 0.03 | 0.04± 0.04 | 0.0116± 0.0011 | 0.26± 0.05 | 0.0135± 0.0018 |
| | all | 0.13± 0.13 | 0.20± 0.23 | 0.0120± 0.0011 | 0.32± 0.09 | 0.0141± 0.0014 |

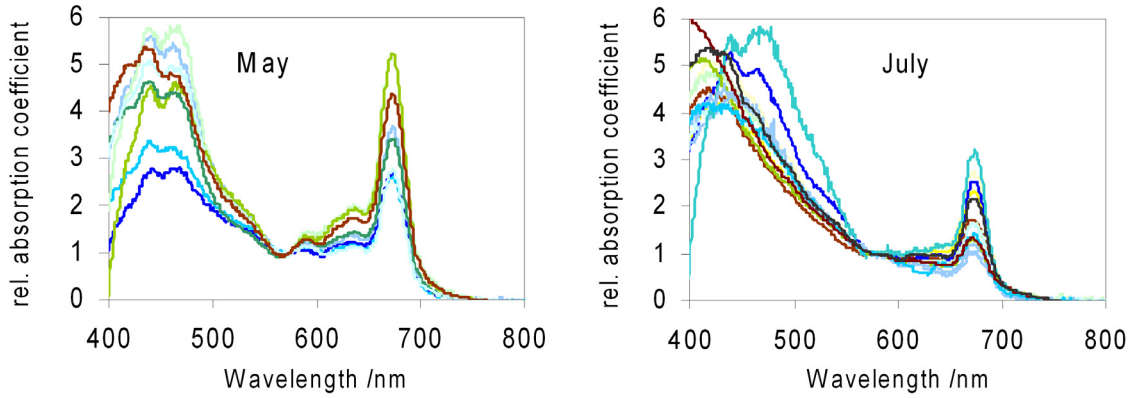


*Figure 2: Phytoplankton absorption coefficient normalised to 575 nm for the May and July cruises. Note the colour code; blue for offshore stations and green-yellow-brown for coastal stations (see Figure 1).*

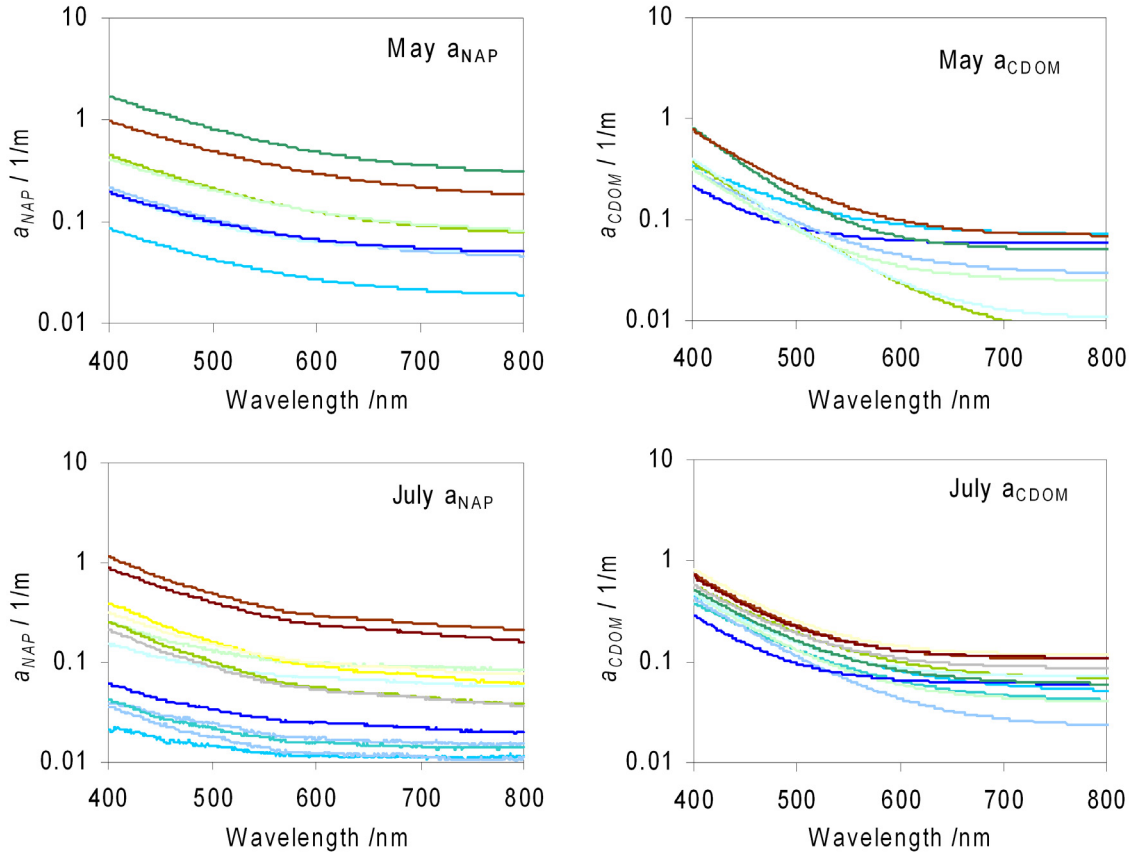


*Figure 3: NAP and CDOM absorption spectra determined during the May and July cruises (fitted data). Note the logarithmic scale to show the differences in the slope of the curves. Note the colour code; blue for offshore stations and green-yellow-brown for coastal stations (see Figure 1).*

Statistical analysis of data in Table 2 reveals that there is no significant variation between coast and offshore for $a_{ph}$ ($p$=0.18) and $a_{CDOM}$ ($p$=0.20), but there is for $a_{NAP}$ ($p$=0.009) during the May cruise. In the July cruise, $a_{ph}$ ($p$=0.002), $a_{NAP}$ (p=0.001) and $a_{CDOM}$ (p=0.016) show significant coast-offshore differences. These results suggest that during the bloom period there is no coast-offshore gradient due to *Phaeocystis* presence across all the area, while during summer time the differences are probably explained by changes in phytoplankton concentration. The overall data show significant seasonal variation for $a_{NAP}$ ($p$=0.004) but not for $a_{ph}$ ($p$=0.22) nor $a_{CDOM}$ (p=0.10). $S_{NAP}$ and $S_{CDOM}$ show no significant variation between coast-offshore for the May ($S_{NAP}$ p=0.31, $S_{CDOM}$ p=0.15) and July cruises ($S_{NAP}$ p=0.21, $S_{CDOM}$ p=0.22), but there is significant seasonal difference in $S_{NAP}$ ($p$=0.001) and $S_{CDOM}$ ($p$=0.007). The seasonal difference in $S_{NAP}$ might be due to different proportions of mineral and organic matter in the particles (6). The average $S_{NAP}$ value for both cruises is 0.011 /nm, a typical value reported for mineral particles (6). Surprisingly, the only significant difference in $S_{CDOM}$ is found at the seasonal scale. It was expected that $S_{CDOM}$ changes with the type of water present, whether it is more influenced by continental or by Atlantic waters, as observed in the Southern Bight of the North Sea (33). The lack of variability could be explained by the lack of sampling stations at low salinity waters.

**Variability in specific inherent optical properties SIOPs**

The average values for CHL-specific phytoplankton absorption at 442 ($a^*_{ph}$(442)) and 664 nm ($a^*_{ph}$(664)) and TSM-specific NAP absorption at 442 nm ($a^*_{NAP}$(442)) are given in Table 3. The variability of SIOPs is not as high as that observed for IOPs. The highest variability is observed in $a^*_{ph}$(442), with July values being higher than those in May. The difference in phytoplankton composition during the cruises could explain this, with the July community being dominated by diatoms of smaller size and at lower concentrations than in May, therefore having a higher specific absorption. Coast-offshore variation is clear in May for all variables and only in $a^*_{NAP}$(442) for the July cruise.

The coast-offshore variability in $a^*_{NAP}(442)$ in July is higher than May probably reflecting a non-homogenous distribution of particles in the area.

*Table 3: Average SIOPs, specific phytoplankton absorption at 442 and 664 nm and specific NAP absorption at 442 nm, for different locations during the May and July cruises. Standard deviations are showing the variability.*

| Cruise | Location | $a^*_{ph}(442)$ / $m^2$/mg CHL | $a^*_{ph}(664)$ / $m^2$/mg CHL | $a^*_{NAP}(442)$ / $m^2$/g TSM |
|---|---|---|---|---|
| May 2004 | Coast | 0.015± 0.004 | 0.011± 0.001 | 0.032± 0.012 |
| | Offshore | 0.036± 0.020 | 0.019± 0.009 | 0.024± 0.015 |
| | all | 0.022± 0.015 | 0.014± 0.007 | 0.026± 0.014 |
| July 2004 | Coast | 0.054± 0.061 | 0.016± 0.017 | 0.027± 0.020 |
| | offshore | 0.051± 0.033 | 0.015± 0.010 | 0.015± 0.009 |
| | all | 0.053± 0.048 | 0.016± 0.014 | 0.021± 0.017 |

Understanding of the SIOP variability is crucial for algorithm calibration. With this purpose we plotted SIOPs in relation with some water components (Figure 4). Clearly, $a^*_{ph}(442)$ and $a^*_{ph}(664)$ depend on CHL concentration with the highest $a^*_{ph}$ values corresponding to offshore stations characterised by low CHL concentrations and the lowest values to coastal stations with high CHL concentrations (Figure 4a,b). A similar trend has been observed by Bricaud et al. (34) and represented by a power function characterised by a negative exponent. The coastal-offshore differences can be explained by the 'package effect' due to changes in pigment composition or cell size distribution, which modify the magnitudes of the main absorption peaks (34). At 664 nm, the package effect is less important than in the blue part of the spectrum. Also the package effect is known to increase from oligotrophic to eutrophic waters, so that it is expected to contribute significantly to changes in $a^*(442)$ in the eutrophic waters of the Belgian coastal zone. When plotting $a^*_{NAP}(442)$ against TSM concentration there is no obvious relation (Figure 4c). An average $a^*_{NAP}(442)$ value of 0.023±0.015 $m^2$/g can be estimated for the observed range of TSM concentration, close to that previously reported for the North Sea (0.033 $m^2$/g) (6).

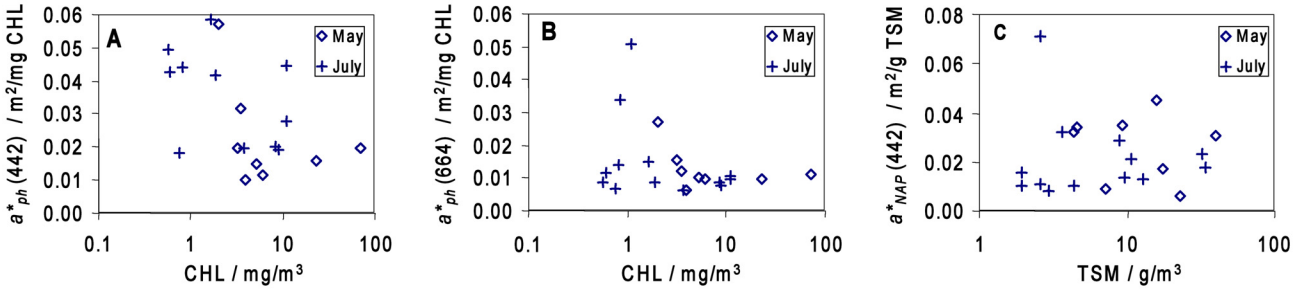


*Figure 4: Scatter plots of SIOPs and some water constituents. A:* $a^*_{ph}$*(442) versus CHL concentration, B:* $a^*_{ph}$*(664) versus CHL concentration and C:* $a^*_{NAP}$*(442) versus TSM concentration.*

No relation between $S_{NAP}$ and TSM is apparent, although $S_{NAP}$ values tend to decrease with increasing TSM (Figure 5). When plotting $S_{CDOM}$ as a function of salinity there is an inverse relation more defined in May, although some outliers are apparent, i.e. stations 700 and 130 with low salinity and station 800 with high salinity. This could result from a different composition of humic and fulvic acids at these stations (31). Stations 700 and 130 are near the coast and are influenced by the Scheldt river discharge so that their CDOM pool is likely to be of terrestrial origin, while station 800 is offshore and more influenced by marine biological production.

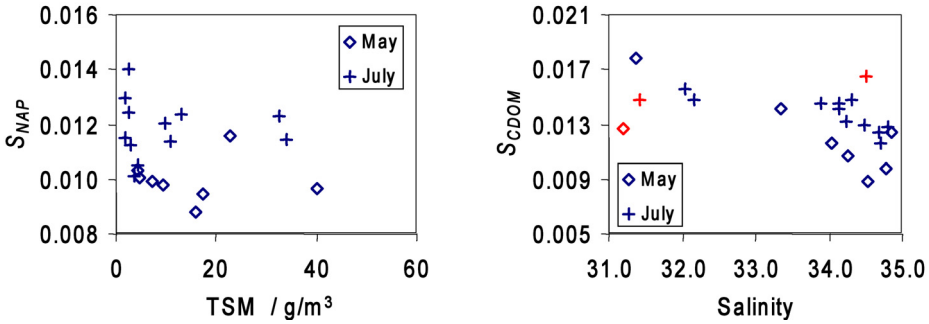


*Figure 5: Scatter plots of $S_{NAP}$ as a function of TSM and $S_{CDOM}$ as a function of salinity for the May and July cruises. In the right hand plot, outliers are highlighted in red.*

**ac-9 results**

Results of total absorption and particle scattering are shown in Figure 6. The total absorption values are higher in spring than in winter and the shape of the spectra reveals that the water is phytoplankton-dominated in spring, while in summer the spectra resemble the shape of CDOM or NAP, indicating that one or both dominate. These results agree with those previously found for phytoplankton absorption, although there are some key wavelengths which are not well represented by ac-9, for example around 460 nm where some carotenoids have their maximum absorption (Figure 6).

The scattering values are high for both seasons (up to 20/m), indicating that the contribution of particles is always important in these waters. The shape of the scattering spectra is variable. In those stations with high contribution of phytoplankton their shape shows lower values around 440 and 676 nm corresponding to the phytoplankton absorption.

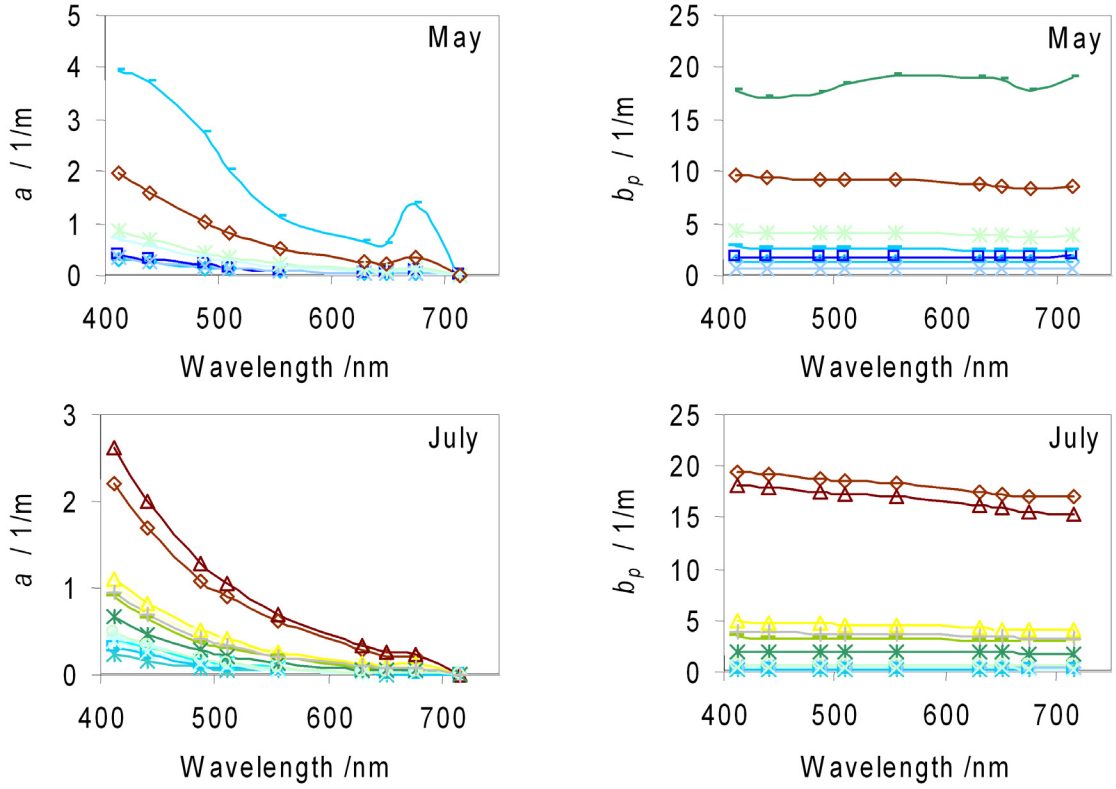


*Figure 6: Results of ac-9 measurements performed during May and July cruises showing total non-water absorption a (particles+dissolved material) and particle scattering $b_p$. Note the colour code; blue for offshore stations and green-yellow-brown for coastal stations (see Figure 1).*

### Reflectance spectra

The reflectance spectra measured during the cruises show a high spatial and temporal variability, with higher values in July than in May. The shapes of the spectra are also different between these cruises, in particular regions between 450-550 nm and 655-700 nm (Figure 7).

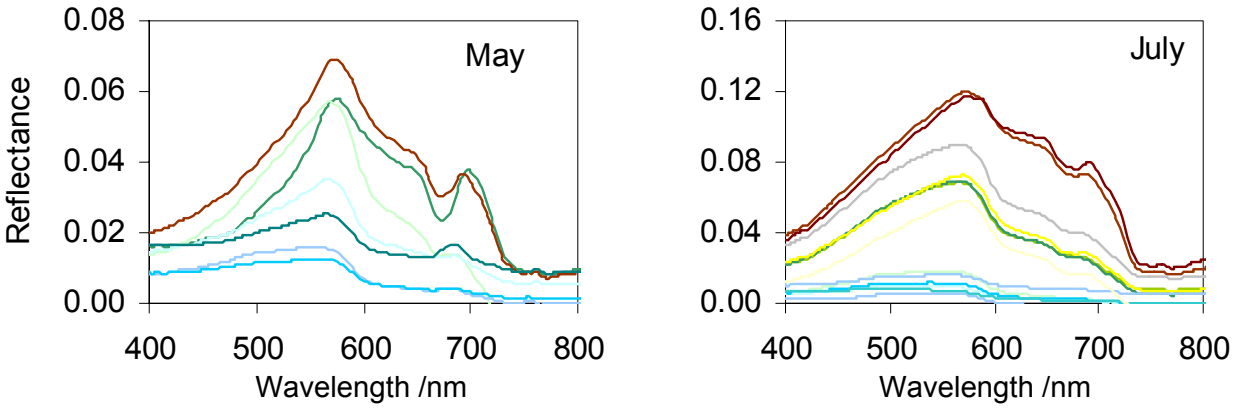


*Figure 7: Reflectance spectra for the May and July cruises. Note the colour code; blue for offshore stations and green-yellow-brown for coastal stations (see Figure 1).*

### Impact of IOP variability on satellite algorithms

The two key questions investigated here regarding the IOP variability impact on satellite algorithms are:

- Does neglecting CDOM and NAP absorption for the red and NIR wavelengths affect CHL retrieval and, if so, can the algorithm be improved?
- How does the assumption of constant CHL-specific phytoplankton absorption coefficient affect accuracy of CHL retrieval and can the algorithm be improved in this respect?

The results of the simulations to assess the impact of CDOM and NAP absorption on CHL retrieval (see Methods section) are shown in Figure 8. The difference between retrieved and input $a_{ph}(664)$ is due to the difference between actually measured $a_{CDOM}^{m}(\lambda)$ and $a_{NAP}^{m}(\lambda)$ at 664, 708 and 778 nm and $a_{ph}^{m}(\lambda)$ at 708 nm and the zero values for these parameters which are assumed in the algorithm development.

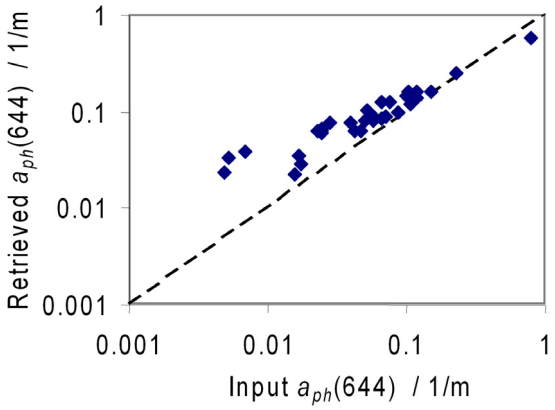


*Figure 8: Scatter plot of input and retrieved $a_{ph}(664)$ showing the impact on algorithm performance of neglecting $a_{CDOM}^{m}(\lambda)$ and $a_{NAP}^{m}(\lambda)$ at 664, 708 and 778 nm and $a_{ph}^{m}(\lambda)$ at 708 and 778 nm (May and July cruises).*

In order to better identify these IOP-related algorithm errors, two further variants were made on these simulations:

a) Setting $a_{CDOM}^{m}(778) = a_{NAP}^{m}(778) = a_{ph}^{m}(778) = 0$ in the input, thus removing any error associated with estimation of $b_b$, and,

b) Setting $a_{CDOM}^{m}(664) = a_{NAP}^{m}(664) = a_{CDOM}^{m}(708) = a_{NAP}^{m}(708) = 0$ in the input, thus removing any error associated with neglecting CDOM and NAP absorption in Eq. (11).

The results of these further simulations are shown in Figure 9.

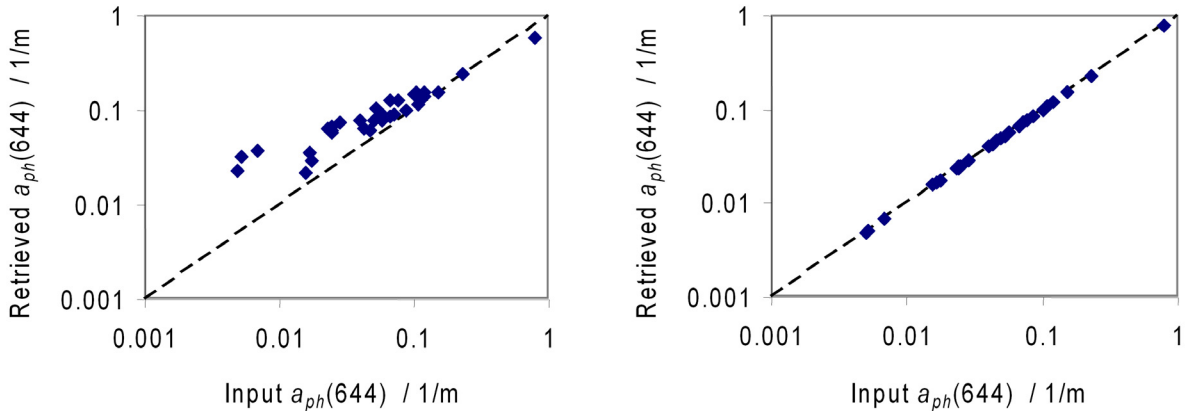


*Figure 9: As Figure 8 but for simulations with Left:* $a_{CDOM}^{m}(778) = a_{NAP}^{m}(778) = a_{ph}^{m}(778) = 0$ *and Right:* $a_{CDOM}^{m}(664) = a_{NAP}^{m}(664) = a_{CDOM}^{m}(708) = a_{NAP}^{m}(708) = 0$.

Comparing Figure 9 (left) with Figure 8 it is clear that results are not greatly improved by setting the input non-water absorption coefficients at 778 nm to zero. Therefore, this is not the main source of algorithm retrieval errors in the simulations of Figure 8. However, setting the input CDOM and NAP absorption at 664 nm and 708 nm to zero gives almost perfect retrieval (Figure 9 right) showing that the error in Figure 8 could be attributed almost entirely to the imperfect assumption that these coefficients are negligible. Theoretically it is easy to derive that non-zero CDOM and NAP absorption at 664 nm and 708 nm gives an error in $a_{ph}(664)$ retrieval of:

$$\varepsilon_{ph}(664) = \left(a_{CDOM}(664) + a_{NAP}(664)\right) - \frac{\rho_w(708)}{\rho_w(664)}\left(a_{CDOM}(708) + a_{NAP}(708)\right) \qquad (16)$$

Since the reflectance ratio in Eq. (16) is of order one and the CDOM and NAP absorption coefficients are generally lower at 708 nm than at 664 nm, it is clear that this error will be generally positive (as seen in Figure 8). This error is also unrelated to the magnitude of $a_{ph}(664)$ and will thus be relatively more important for low CHL.

In this analysis, it is assumed that the CDOM and NAP measurements used are free of error. CDOM measurements are highly affected by temperature effects in the NIR part of the spectrum (21). It is known that a temperature difference of 1°C leads to an increase in water absorption of 0.009/m at 750 nm. If there is a temperature difference between reference and sample during the CDOM measurement, this will lead to an increase in absorption. In our protocol, samples are allowed to reach room temperature before the measurement to avoid this problem. However, there could be a small temperature difference that has not been taken into account and could lead to an overestimation of the CDOM values in the NIR. If, for example, CDOM absorption measurements are overestimated, then the retrieval error shown in Figure 9 would be overestimated as can be seen by changing these values in Eq. (16). A series of parallel simulations were made supposing that the measured values are indeed overestimated. If 30% or 70% are removed from the measured CDOM in the NIR, the retrieved $a_{ph}(664)$ decreases by 14% and 34%, respectively. Results show that the retrieved $a_{ph}(664)$ decrease by 23% of its original value if the measured $a_{CDOM}$ values are overestimated by 70%, so the error in the retrieval decreases, too (Figure 10). Thus, overestimation of CDOM absorption in the measurements may lead to some exaggeration in the CHL retrieval error caused by neglecting this absorption in the algorithm design (Figure 9). However, it is clear from these results and from the simple theoretical analysis of Eq. (16) that neglecting CDOM

and NAP absorption for red/NIR CHL retrieval algorithms will lead to a significant error for low CHL and high CDOM or NAP conditions.

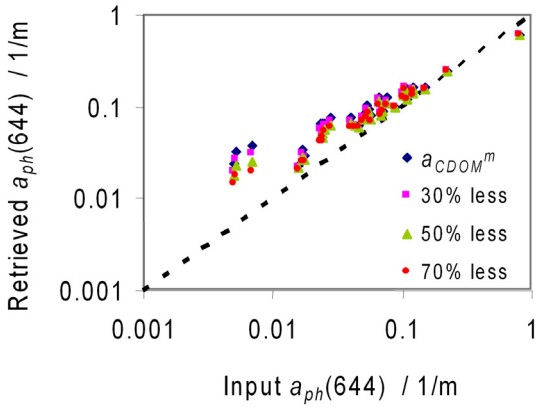


*Figure 10: Scatter plot of input and retrieved $a_{ph}(664)$ showing the impact on algorithm performance of the overestimation of $a_{CDOM}^{m}$ in the NIR (May and July cruises). In blue the $a_{CDOM}^{m}$ and in colour the decrease of these values in percentages.*

**Variability of CHL-specific phytoplankton absorption**

Since the CHL-retrieval algorithm retrieves essentially the phytoplankton absorption coefficient, it is obvious from Eq. (13) that any variability in the SIOP $a^*_{ph}(664)$ will proportionally impact the derived chlorophyll products. This cannot explain the poor retrievals observed for low CHL in previous studies, but is probably one of the most significant sources of error for the high CHL retrievals.

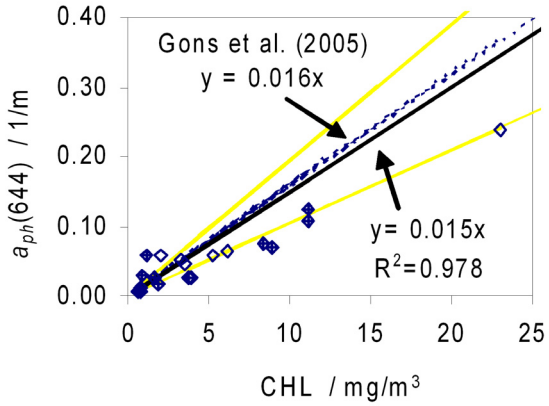


*Figure 11: Scatter plot of $a_{ph}(664)$ as a function of CHL. The thick line represents the linear relation between the data and the yellow lines represent the 30% error lines. Also shown is the Gons et al. (2005) calibration $a_{ph}(664)=0.016*CHL$ in dashed lines. Open squares correspond to the May cruise and filled squares to the July cruise.*

Figure 11 shows the variability of $a_{ph}(664)$ as a function of CHL concentration. The relation is linear with a good fit, although some dispersion of the data is observed at low CHL values (<5 mg/m$^3$). A previous study found that this relation can be represented by a power law for case 1 water (34). The phytoplankton absorption at 664 nm varies between cruises, being higher on average in May (0.170/m) than in July (0.043/m). The overall variability in $a_{ph}(664)$ can be explained by differences in pigment composition and package effect (which varies the ratio 442/664 nm) between cruises (29,34), with large *Phaeocystis* colonies (1-2 mm) in May and small cells (20-200 μm) in July. Not only the size but the abundance of cells in the water during May could explain the high value of absorption compared with July when the abundance is less and also the cell size decreases. It can be seen from Figure 11 that the overall average value for $a^*_{ph}(664)$ in this study (0.015±0.011 m$^2$/mg CHL) is very close to that from (26), confirming the similar characteristics of the phytoplankton populations between the sites.

## CONCLUSIONS

The overall variability of IOPs measured in the area was found to be high for $a_{ph}(442)$ and $a_{NAP}(442)$ but not for $a_{CDOM}(442)$. $S_{NAP}$ and $S_{CDOM}$ showed only limited variability. The variability of SIOPs was found to be high for $a^*_{ph}(442)$ but not for $a^*_{ph}(664)$ nor $a^*_{NAP}(442)$. NIR absorption measurements confirm that there is significant NIR absorption for NAP and possibly also for CDOM, though measurement uncertainties may be significant for the latter.

The absorption coefficient measurements have been used to evaluate the error associated with neglecting NIR absorption from NAP and CDOM in the CHL-retrieval algorithm for high CHL, high TSM waters based on wavelengths 664, 708 and 778 nm (26).

Simulations using the measured phytoplankton, NAP and CDOM absorption coefficients show that the consequence of neglecting NAP and CDOM absorption at 664 and 708 nm is an overestimation of CHL as suggested by Gons et al. (10). This overestimation is supported theoretically and is shown to be independent of CHL, thus most significant in relative terms for low CHL. This is one important source of error for this algorithm at low CHL, along with the error associated with reflectance measurements in low NIR reflectance waters considered previously by Ruddick et al. (14). Algorithm improvements could possibly be achieved by estimation of NIR CDOM and NAP absorption either *a priori* from knowledge of the region or from retrieval of the CDOM+NAP absorption coefficient from reflectance at other wavelengths.

A second important source of error for this CHL-retrieval algorithm, and for any other CHL-retrieval algorithm based on retrieval of phytoplankton absorption and conversion from absorption to CHL, is the use of a fixed $a^*_{ph}$. This was effectively calibrated from reflectance measurements in the original algorithm. By direct measurement of $a^*_{ph}(664)$ it was found that this SIOP varies between 0.004-0.026 $m^2$/mg CHL which propagates directly into a corresponding error in CHL retrieval and is thus a key source of error in CHL retrieval. The measurements reported here will be supplemented by more data measured for different phytoplankton species, regions and seasons in order to determine whether it is possible to characterise variability of this SIOP and hence vary this parameter appropriately in retrieval algorithms.

For processing of satellite imagery multispectral algorithms are now emerging (35,36,37) which invert the reflectance spectra to simultaneously retrieve a number of optical constituents, for example, phytoplankton and CDOM absorption and particulate backscatter, or similarly a number of parameters such as CHL, CDOM and/or NAP absorption and TSM. Such algorithms implicitly contain and use the extra information needed for taking account of CDOM and NAP absorption when retrieving CHL. However, such use of retrieved CDOM or NAP absorption requires that these parameters be accurately retrieved, which may not always be possible. An alternative or possibly complementary approach for the future could be to use regional climatologies or maps of typical values for CDOM and NAP absorption with spatial and possibly seasonal variability as auxiliary data for CHL retrieval. For each pixel of a satellite image the CHL retrieval algorithm could use auxiliary information for the expected CDOM and NAP absorption coefficients at the required wavelength in a second order correction of the basic algorithm. Thus, the limited information available in satellite reflectance measurements can be mitigated by use of auxiliary information. In a similar way it may be possible to build up maps, possibly seasonally varying, of $a^*_{ph}$, although for such an approach research is still needed to characterise the variability of this crucial SIOP.

## ACKNOWLEDGEMENTS

This study was funded by the STEREO programme of the Belgian Federal Science Policy Office in the framework of the BELCOLOUR project. The captain and crew of the Research Vessel Belgica are thanked for their assistance with seaborne measurements. The staff at MUMM/Oostende laboratory are acknowledged for providing the CHL concentrations. Two anonymous referees are thanked for giving helpful comments improving the manuscript.

## REFERENCES


1 OSPAR, 2003. Rapport intégré OSPAR de 2003 sur l'état d'eutrophisation de la zone maritime OSPAR, basé sur la première application de la Procédure exhaustive. 56 pp.

2 Van Bennekom A J & F J Wetsteijn, 1990. The winter distribution of nutrients in the Southern Bight of the North Sea (1961-1978) and in the estuaries of the Scheldt and the Rhine/Meuse. Netherlands Journal of Sea Research, 25(1/2): 75-87

3 Lancelot C, G Billen, A Sournia, T Weisse, F Colijn, M J W Veldhuis, A Davies & P Wassman, 1987. *Phaeocystis* blooms and nutrient enrichment in the continental coastal zones of the North Sea. Ambio, 16(1): 38-46

4 Fettweis M & D Van Den Eynde, 2003. The mud deposits and the high turbidity in the Belgian-Dutch coastal zone, Southern Bight of the North Sea. Continental Shelf Research, 23: 669-691

5 Belcolour website: http://www.mumm.ac.be/BELCOLOUR

6 Babin M, D Stramski, G M Ferrari, H Claustre, A Bricaud, G Obolensky & N Hoepffner, 2003. Variations in the light absorption coefficients of phytoplankton, nonalgal particles, and dissolved organic matter in coastal waters around Europe. Journal of Geophysical Research, 108(C7): 3211. doi:10.1029/2001JC000882

7 Peters S W M, M Eleveld, R Pasterkamp, H van der Woerd, M de Volder, S Jans, Y Park, K Ruddick, T Block, C Brockmann, R Doerffer, H Krasemann, W Schoenfeld, P V Jørgenson, G Tilstone, G Moore, K Sørensen, J Hokedal & E Aas, 2005. Atlas of Chlorophyll-a concentration for the North Sea based on MERIS imagery of 2003 (Vrije Universiteit, Amsterdam) 121 pp.

8 Dekker A G, 1993. Detection of water quality parameters for eutrophic waters by high resolution remote sensing. PhD thesis (Vrije Universiteit Amsterdam) 222 pp.

9 Gons H J, 1999. Optical teledetection of chlorophyll-a in turbid inland waters. Environmental Science and Technology, 33: 1127-1133

10 Gons H J, M Rijkeboer & K G Ruddick, 2002. A chlorophyll-retrieval algorithm for satellite imagery (Medium Resolution Imaging Spectrometer) of inland and coastal waters. Journal of Plankton Research, 24: 947-951

11 Mittenzwey K H, A A Gitelson, S Ullrich & K Y Kondratiev, 1992. Determination of chlorophyll a of inland waters on the basis of spectral reflectance. Limnology and Oceanography, 37: 147-149

12 De Cauwer V, K Ruddick, Y Park, B Nechad & M Kyramarios, 2004. Optical remote sensing in support of eutrophication monitoring in the Southern North Sea. EARSeL eProceedings, 3: 208-221

13 Gons H J, M Rijkeboer, S Bagheri & K G Ruddick, 2000. Optical teledetection of chlorophyll-*a* in estuarine and coastal waters. Environmental Science and Technology, 34: 5189-5192

14 Ruddick K G, H J Gons, M Rijkeboer & G Tilstone, 2001. Optical remote sensing of chlorophyll-*a* in case 2 waters using an adaptive two-band algorithm with optimal error properties. Applied Optics, 40: 3575-3585

15 Tassan S & G Ferrari, 1995. An alternative approach to absorption measurements of aquatic particles retained on filters. Limnology and Oceanography, 40(8): 1358-1368

16 Tassan S & G M Ferrari, 2002. A sensitivity analysis of the 'Transmittance-Reflectance' method for measuring light absorption by aquatic particles. Journal of Plankton Research, 24(8): 757-774

17 Tassan S & G Ferrari, 1998. Measurement of light absorption by aquatic particles retained on filters: determination of the optical pathlength amplification by the 'transmittance-reflectance' method. Journal of Plankton Research, 20(9): 1699-1709

18 Ferrari G & S Tassan, 1999. A method using chemical oxidation to remove light absorption by phytoplankton pigments. Journal of Phycology, 35: 1090-1098

19 Tassan S & G M Ferrari, 2003. Variability of light absorption by aquatic particles in the near-infrared spectral region. Applied Optics, 42(24): 4802-4810

20 Tilstone G, G F Moore, K Sørensen, R Doerffer, R Røttgers, K G Ruddick, R Pasterkamp & P V Jørgensen, 2002. REVAMP, Regional Validation of MERIS Chlorophyll products in North Sea coastal waters. Protocols, 68 pp.

21 Pegau W S, G Deric & J R V Zaneveld, 1997. Absorption and attenuation of visible and near-infrared light in water: Dependence on temperature and salinity. Applied Optics, 36: 6035-6046

22 Zaneveld J R V, R Bartz & C M Moore, 1994. The scattering error correction of reflecting-tube absorption meters. Proceedings SPIE, Ocean Optics XII, 2258: 44-55

23 Twardowski M S, J M Sullivan, P L Donaghay & J R V Zaneveld, 1999. Microscale quantification of the absorption by dissolved and particulate material in coastal waters with an ac-9. Journal of Atmospheric and Oceanic Technology, 16(12): 691-707

24 Mueller J L, C Davis, R Arnone, R Frouin, K Carder, Z P Lee, R G Steward, S Hooker, C D Mobley & S McLean, 2000. Above-Water Radiance and Remote Sensing Reflectance Measurement and Analysis Protocols. In: Ocean Optics Protocols for Satellite Ocean Color Sensor Validation, Revision 2, edited by G S Fargion & J L Mueller (NASA) 98-107

25 Ruddick K G, V De Cauwer, Y Park & G Moore, 2006. Seaborne measurements of near infrared water-leaving reflectance - the similarity spectrum for turbid waters. Limnology and Oceanography (in press)

26 Gons H J, M Rijkeboer & K G Ruddick, 2005. Effect of a waveband shift on chlorophyll retrieval from MERIS imagery of inland and coastal waters. Journal of Plankton Research, 27: 125-127

27 Gordon H R, O B Brown, R H Evans, J W Brown, R C Smith, K S Baker & D K Clark, 1988. A semianalytical radiance model of ocean color. Journal of Geophysical Research, 93: 10909-10924

28 Buiteveld H, J M.H Hakvoort & M Donze, 1994. The optical properties of pure water. In: Proceedings of Ocean Optics XII, edited by J S Jaffe (SPIE) 174-183

29 Stuart V, S Sathyendranath, E J Head, T Platt, B Irwin & H Maass, 2000. Bio-optical characteristics of diatom and prymnesiophyte populations in the Labrador Sea. Marine Ecology Progress Series, 201: 91-106

30 Jeffrey S W, R F C Mantoura & S W Wright (Editors), 1997. Phytoplankton pigments in oceanography, guidelines to modern methods (UNESCO Publishing, Paris, France) Vol. 10, 661 pp.

31 Stedmon C A & S Markager, 2001. The optics of chromophoric dissolved organic matter (CDOM) in the Greenland Sea: An algorithm for differentiation between marine and terrestrially derived organic matter. Limnology and Oceanography, 46(8): 2087-2093

32 Babin M & D Stramski, 2002. Light absorption by aquatic particles in the near-infrared spectral region. Limnology and Oceanography, 47(3): 911-915

33 Warnock R E, W W C Gieskes & S Van Laar, 1999. Regional and seasonal differences in light absorption by yellow substance in the Southern Bight of the North Sea. Journal of Sea Research, 42: 169-178

34 Bricaud A, M Babin, A Morel & H Claustre, 1995. Variability in the chlorophyll-specific absorption coefficients of natural phytoplankton: Analysis and parameterization. Journal of Geophysical Research, 100(C7): 13321-13332

35 Vasilkov A P, 1997. A retrieval of coastal water constituent concentrations by least-square inversion of a radiance model. 4th International Conference on Remote Sensing for Marine and Coastal Environment (Environmental Research Institute of Michigan, Ann Arbor, Mich.) 107-116

36 Schiller H & R Doerffer, 1999. Neural network for emulation of an inverse model operational derivation of Case II water properties from MERIS data. International Journal of Remote Sensing, 20: 1735-1746

37 Dekker A G, V E Brando, J M Anstee, N Pinnel, T Kutser, E J Hoogenboom, S Peters, R Pasterkamp, R Vos, C Olbert & T J M Malthus, 2001. Imaging Spectrometry of Water. In: Imaging Spectrometry, edited by F. D. Van der Meer and S. M. de Jong (Kluver) 307-359